J Biol Phys (2008) 34:91–106
DOI 10.1007/s10867-008-9109-9

ORIGINAL PAPER

Robustness in *Escherichia coli* Glutamate and Glutamine Synthesis Studied by a Kinetic Model

Aníbal Lodeiro · Augusto Melgarejo

Received: 18 October 2007 / Accepted: 28 July 2008 /
Published online: 30 August 2008

Abstract Metabolic control of glutamine and glutamate synthesis from ammonia and oxoglutarate in *Escherichia coli* is tight and complex. In this work, the role of glutamine synthetase (GS) and glutamate dehydrogenase (GDH) regulation in this control was studied. Both enzymes form a linear pathway, which can also have a cyclic topology if glutamate–oxoglutarate amino transferase (GOGAT) activity is included. We modelled the metabolic pathways in the linear or cyclic topologies using a coupled nonlinear differential equations system. To simulate GS regulation by covalent modification, we introduced a relationship that took into account the levels of oxoglutarate and glutamine as signal inputs, as well as the ultrasensitive response of enzyme adenylylation. Thus, by including this relationship or not, we were able to model the system with or without GS regulation. In addition, GS and GDH activities were changed manually. The response of the model in different stationary states, or under the influence of N-input exhaustion or oscillation, was analyzed in both pathway topologies. Our results indicate a metabolic control coefficient for GDH ranging from 0.94 in the linear pathway with GS regulation to 0.24 in the cyclic pathway without regulation, employing a default GDH concentration of 8 μM. Thus, in these conditions, GDH seemed to have a high degree of control in the linear pathway while having limited influence in the cyclic one. When GS was regulated, system responses to N-input perturbations were more sensitive, especially in the cyclic pathway. Furthermore, we found that effects of regulation against perturbations depended on the relative values of the glutamine and glutamate output first-order kinetic constants, which we named k_6 and k_7, respectively. Effects of regulation grew exponentially with a factor around 2, with linear increases of $(k_7 - k_6)$. These trends were sustained but with lower differences at higher GS

A. Lodeiro (✉)
Instituto de Bioquímica y Biología Molecular (IBBM),
Departamento de Ciencias Biológicas, Facultad de Ciencias Exactas,
Universidad Nacional de La Plata, Calles 47 y 115, 1900 La Plata, Argentina
e-mail: lodeiro@biol.unlp.edu.ar

A. Melgarejo
Área Departamental Ciencias Básicas, Facultad de Ingeniería,
Universidad Nacional de La Plata, Calles 1 y 47, 1900 La Plata, Argentina

concentration. Hence, GS regulation seemed important for metabolic stability in a changing environment, depending on the cell's metabolic status.

Keywords Glutamine synthetase · Pathway topology · Regulation · Metabolic control · Kinetic model

1 Introduction

The biosynthesis of glutamate (E) and glutamine (Q) from NH_4^+ as N-source and 2-oxoglutarate (OG) as C-skeleton source in prokaryotes holds a key position among metabolic processes. It links N incorporation to all cellular components with tricarboxylic acids cycle, a main pathway for aerobic energy production and C-skeleton synthesis for diverse biological compounds. Therefore, regulation of this N-assimilatory pathway must be very accurate in order to preserve the necessary balance among the cell's C, N and energy demands.

In *Escherichia coli*, three enzymes catalyze the reactions of this pathway (Fig. 1). Glutamate dehydrogenase (GDH, EC 1.4.1.4) catalyzes the reductive amination of OG with NH_4^+ to give E in a single step using nicotinamide adenosine dinucleotide phosphate (NADPH) as electron donor. This enzyme has relatively high K_M values for both substrates. Furthermore, glutamine synthetase (GS, EC 6.3.1.2) uses E and a second NH_4^+ molecule to produce Q, consuming 1 mol of adenosine triphosphate (ATP) per mole of Q produced. On the other hand, GS integrates a cycle with glutamine–oxoglutarate amino transferase (GOGAT, EC 1.4.1.13, also known as glutamate synthase), which also produces E, this time using Q and OG as substrates. Hence, E biosynthesis can be achieved in two ways: GDH reaction or GS/GOGAT cycle, while Q may be synthesized in a linear GDH-GS pathway, or it can also be obtained from the GS/GOGAT cycle. Therefore, for both amino acids, two

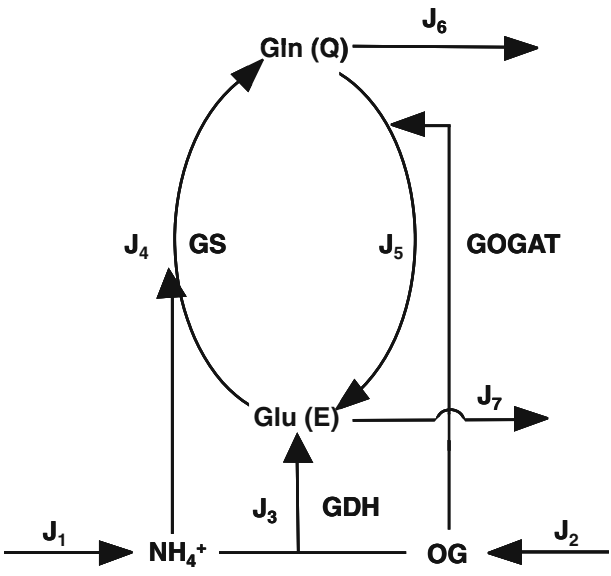

Fig. 1 Schematic representation of the E and Q production pathways. In the linear topology, the reaction catalyzed by GOGAT (J_5) was removed

alternative routes may coexist: a linear pathway with the participation of GDH, or a cyclic pathway with the additional participation of GOGAT. Since E biosynthesis through the cyclic pathway always involves the ATP-consuming GS reaction, this pathway is, in general, more expensive in terms of ATP consumption and, as a whole, possesses lower K_M values for the substrates OG and NH_4^+ (for a review, see [1]).

All three enzymes were purified and fully characterized four decades ago, and the control of expression of genes encoding them is also well known. Of particular interest is the complex regulation of GS since, in contrast to the other enzymes in the pathway, it is subjected to allosteric regulation and covalent modification, in addition to gene expression regulation [2]. As in many other examples in metabolism, such a tight regulation of enzyme activity occurs at the energy-consuming step, and thus, this reaction could be a main control point for the whole flux in this pathway.

GS is a dodecamer of 12 identical subunits. Each subunit may be covalently modified by adenylylation at a specific tyrosine residue in response to the intracellular OG/Q (C/N) ratio, the modified subunits becoming inactive. The adenylylation state of each subunit seems not to condition the state of the others, and in this sense, each subunit is modified independently. While low C/N ratios indicate N abundance and promote adenylylayion (inactivation) of GS, high C/N ratios promote GS deadenylylation (activation). Thus, GS-AMP_{12} can be considered as completely inactive. In addition, adenylylation of each GS subunit renders GS more sensitive to allosteric inhibition by several metabolites, including products of Q metabolism [3, 4]. A recent in silico study of GS regulation indicated that covalent modification accounts for 60% of total regulation and, therefore, can be considered as the main response of the system against changes in C/N ratio [5].

Sensing of C/N ratio for GS adenylylation is carried out by a bicyclic cascade where the protein PII plays a central role [6]. PII is a trimeric protein that may exist in two forms: uridylylated (PII∼UMP) or deuridylylated (PII). Uridylylation takes place at each subunit as catalyzed by a urydylyl-transferase/uridylyl-removing enzyme (UT/UR) [7] according to the Q concentration inside the cell: high Q concentrations promote UR, while low Q concentrations promote UT. On the other hand, OG can directly bind to PII depending on the protein uridylylation state. Unmodified PII binds OG to each subunit with negative cooperativity, while PII uridylylation reduces this negative cooperativity, and thus, less OG concentration is required to saturate PII∼UMP binding sites [6]. PII is able to interact with another modifying/demodifying enzyme, giving rise to the second step of the cascade. This enzyme has adenylyl-transferase/adenylyl-removing activities (AT/AR), which are exerted on GS. When PII is unmodified and with OG bound to only one subunit, it induces AT activity, thus inactivating GS in response to a low C/N intracellular ratio. Conversely, PII∼UMP, with its three subunits saturated with OG, induces AR activity and, therefore, activates GS in response to a high intracellular C/N ratio.

This bicyclic cascade has been proven as robust since variation in the concentration of its components did not alter the response [8, 9]. Although ambiguous modifying enzymes like AT/AR and UT/UR were regarded as lacking ultrasensitivity in their response [8], allosteric regulation in PII and GS seems to provide robustness and ultrasensitivity with a Hill coefficient of around 2 [9].

Regulation of GS has been thought of as a means to ensure Q provision under N scarcity given its low K_M for NH_4^+ and its increasing activation rate with increases in C/N ratio. However, regulation of this enzyme seems exceedingly complex for that adaptation alone, for which gene regulation would suffice, as is the case with other enzymes catalyzing biosynthesis of elementary biological molecules. Instead, this complex and ultrasensitive

regulation might serve to coordinate C and N metabolic demands in a changing environment where supplies of one or both of these nutrients may vary over short time periods.

In addition, the role of superimposed cyclic GS/GOGAT and linear GDH pathways is still unclear. Studies with mutant strains suggested that GDH would be used under nutrient-abundance and energy-limiting conditions since it is able to provide E at a lower ATP expense than the GS-GOGAT pathway [10, 11]. However, both GDH and GOGAT seem to be present at the same time, and therefore, both enzymes compete for OG. Since GOGAT has a $K_M \sim 100$ times lower for this metabolite, OG concentration should be, in principle, quite high for significant GDH activity (Fig. 1). GDH is also placed at the beginning of both pathways. In other metabolic pathways, the total activity of the first enzyme in the pathway may exert a significant control on pathway flux. However, no studies were carried out to assess the possible control ability of GDH.

Here, we tried to better understand the role of GS regulation and GDH activity in the metabolic control of this pathway under changing C and N availabilities, as well as how the simultaneous presence of GDH and GOGAT might affect E and Q production. To this end, we developed a kinetic model where regulated and unregulated GS enzymes were compared, GDH amounts were varied, and different pathway topologies exchanging mass with the exterior were used (Fig. 1). We focused our study of GS regulation on covalent modification ultrasensitivity by applying a relation that estimates the mean fraction of adenylylated GS subunits per dodecamer [9]. This relation considers intracellular concentrations of OG and Q as input variables. Therefore, we could not apply the above-mentioned in silico model to evaluate the effects of GS covalent modification under nonstationary state conditions because, in that model, OG and NH_4^+ concentrations were held fixed [5]. Therefore, we developed a simpler and more restricted model that considered only GS covalent modification for GS regulation, and all metabolite concentrations were allowed to vary.

2 Materials and Methods

2.1 Pathway Topology and Stoichiometry

The system outlined in Fig. 1 was employed with two different topologies, namely, the cyclic topology – as in Fig. 1 – or the linear topology—where the reaction catalyzed by GOGAT was removed. Therefore, the pathway can be described in terms of the following stoichiometry equations:

For the cyclic topology (full pathway):

$$\text{outside} \xrightarrow{J_1} 3NH_4^+$$

$$\text{outside} \xrightarrow{J_2} 2OG$$

$$OG + NH_4^+ \xrightarrow{J_3} E$$

$$2NH_4^+ + 2E \xrightarrow{J_4} 2Q$$

$$Q + OG \xrightarrow{J_5} 2E$$

$$Q \xrightarrow{J_6} \text{outside}$$

$$E \xrightarrow{J_7} \text{outside}$$

For the linear topology (without GOGAT):

$$\text{outside} \xrightarrow{J_1} 3\text{NH}_4^+$$

$$\text{outside} \xrightarrow{J_2} 2\text{OG}$$

$$2\text{OG} + 2\text{NH}_4^+ \xrightarrow{J_3} 2\text{E}$$

$$\text{NH}_4^+ + \text{E} \xrightarrow{J_4} \text{Q}$$

$$J_5 = 0$$

$$\text{Q} \xrightarrow{J_6} \text{outside}$$

$$\text{E} \xrightarrow{J_7} \text{outside}$$

The pairs [adenosine diphosphate (ADP) + Pi/ATP] and [$NADP^+ + H^+$/NADPH] were considered as internal to the system, with constant concentrations [9], as follows (in mM): ATP, 5.0; ADP, 1.0; phosphate (Pi), 10.0; NADPH, 0.15; and NADP, 0.05 [5].

2.2 Calculation of Fluxes and Metabolite Concentrations

The magnitudes J_3, J_4, and J_5 represent the internal J_i fluxes in the system, whose sum gives:

$$3NH_4^+ + 2OG \rightarrow E + Q$$

which are compensated by the J_e external fluxes J_1, J_2, J_6, and J_7. All J_i values were calculated by applying previously described kinetic equations [5, 12], considering the reactions catalyzed by GDH and GS as reversible, and GOGAT-catalyzed reaction as almost irreversible [13]. Hence, each J_i value was calculated as:

$$J_3 = \frac{\dfrac{[\text{GDH}]\,k_{\text{cat},3}}{K_{M3,\text{NH}_4^+} K_{M3,\text{OG}} K_{M3,\text{NADPH}}} \left(\left[\text{NH}_4^+\right][\text{OG}][\text{NADPH}] - \dfrac{[\text{E}][\text{NADP}]}{K_{eq,3}} \right)}{\left(1 + \dfrac{\left[\text{NH}_4^+\right]}{K_{M3,\text{NH}_4^+}}\right)\left(1 + \dfrac{[\text{OG}]}{K_{M3,\text{OG}}} + \dfrac{[\text{E}]}{K_{M3,\text{E}}}\right)\left(1 + \dfrac{[\text{NADPH}]}{K_{M3,\text{NADPH}}} + \dfrac{[\text{NADP}]}{K_{M3,\text{NADP}}}\right)} \tag{1}$$

$$J_4 = \frac{\dfrac{[\text{GS}]\,k_{\text{cat4}}}{K_{M,\text{ATP}} K_{M4,\text{NH}_4^+} K_{M4,\text{E}}} \left([\text{ATP}]\left[\text{NH}_4^+\right][\text{E}] - \dfrac{[\text{ADP}][\text{Q}][\text{P}]}{K_{eq1}} \right)}{\left(1 + \dfrac{[\text{ATP}]}{K_{\text{ATP}}} + \dfrac{[\text{ADP}]}{K_{\text{ADP}}} + \dfrac{[\text{Pi}]}{K_{\text{Pi}}} + \dfrac{[\text{ADP}][\text{Pi}]}{K_{\text{ADP}} K_{\text{Pi}}}\right)} \times$$

$$\times \frac{1}{\left(1 + \dfrac{\left[\text{NH}_4^+\right]}{K_{M4,\text{NH}_4^+}} + \dfrac{[\text{Q}]}{K_{M4,\text{Q}}} + \dfrac{[\text{E}]}{K_{M4,\text{E}}} + \dfrac{[\text{Q}]\left[\text{NH}_4^+\right]}{k_{M4,\text{Q}} K_{N4}} + \dfrac{[\text{E}]\left[\text{NH}_4^+\right]}{K_4 K_{M4,\text{NH}_4^+}}\right)} \tag{2}$$

$$J_5 = \frac{\dfrac{k_{cat,}\, K_{M4,\text{NH}_4^+} K_{M4,\text{E}}}{K_{M2,\text{Q}} K_{M2,\text{OG}}} [\text{GOGAT}][\text{Q}][\text{OG}][\text{NADPH}]}{\left(1 + \dfrac{[\text{Q}]}{K_{M5,\text{Q}}} + \dfrac{[\text{E}]}{K_{M5,\text{E}}}\right)\left(1 + \dfrac{[\text{OG}]}{K_{M5,\text{OG}}} + \dfrac{[\text{E}]}{K_{M5,\text{E}}}\right)\left(1 + \dfrac{[\text{NADPH}]}{K_{M5,\text{NADPH}}} + \dfrac{[\text{NADP}]}{K_{M5,\text{NADP}}}\right)} \tag{3}$$

The input fluxes are defined in Section 3. The output fluxes are defined for both topologies as: $J_6 = k_6\,[\mathrm{Q}]$, $J_7 = k_7\,[\mathrm{E}]$, where k_6 and k_7 are first-order kinetic constants whose values are defined for each simulation in Section 3.

With these fluxes and stoichiometry relationships, matrices were constructed to obtain a system of coupled differential equations expressing J values as time functions for all metabolite concentrations.

The set of differential equations used to represent the instantaneous concentrations of each metabolite, as well as the internal fluxes, depended on the particular topology. For the cyclic topology, the instantaneous concentrations were calculated by the following differential equations [14–16]:

$$\frac{d\,[\mathrm{E}]}{dt} = J_3 - 2J_4 + 2J_5 - J_7,$$

$$\frac{d\,[\mathrm{Q}]}{dt} = 2J_4 - J_5 - J_6,$$

$$\frac{d\,[\mathrm{OG}]}{dt} = -J_3 - J_5 + 2J_2,$$

$$\frac{d\left[\mathrm{NH_4^+}\right]}{dt} = -J_3 - 2J_4 + 3J_1.$$

In turn, for the linear topology, the instantaneous concentrations were calculated as:

$$\frac{d\,[\mathrm{E}]}{dt} = 2J_3 - J_4 - J_7,$$

$$\frac{d\,[\mathrm{Q}]}{dt} = J_4 - J_6,$$

$$\frac{d\,[\mathrm{OG}]}{dt} = -2J_3 + 2J_2,$$

$$\frac{d\left[\mathrm{NH_4^+}\right]}{dt} = -2J_3 - J_4 + 3J_1.$$

Coefficient values used in these equations were obtained from the literature and are listed in Table 1.

2.3 Enzyme Regulation

To assess the influence of gene expression on total GDH or GS activity, total enzyme concentrations were changed manually. In addition, total GS activity was associated with the fraction f of adenylylated subunits per dodecamer. For simplicity, we considered each unmodified subunit as fully active, and each adenylylated one as totally inactive.

Values of f were obtained according to Mutalik et al. [9] from the concentrations of OG and Q as:

$$f = \frac{[\mathrm{Q}]^2}{K_{0.5}^2 + [\mathrm{Q}]^2} \tag{4}$$

Table 1 Parameters used in this study

Enzyme	Parameter	Value	Reference
GS	Concentration	240 nM	[23]
	kcat	1.6 10^6 min^{-1}	[23]
	$K_{M,E}$	4.1 mM	[5]
	K_{M,NH_4^+}	0.1 mM	[5]
	$K_{M,ATP}$	0.35 mM	[5]
	$K_{M,Q}$	5.65 mM	[5]
	$K_{M,ADP}$	0.0585 mM	[5]
	$K_{M,Pi}$	3.7 mM	[5]
	Keq	460	[5]
GOGAT	Concentration	130 nM	[13]
	kcat	2.1 10^4 min^{-1}	[13]
	$K_{M,Q}$	0.175 mM	[5]
	$K_{M,OG}$	0.007 mM	[5]
	$K_{M,NADPH}$	0.0015 mM	[5]
	$K_{M,E}$	11.0 mM	[5]
	$K_{M,NADP}$	0.0037 mM	[5]
GDH	Concentration	8,000 nM	[24]
	kcat	5.3 10^4 min^{-1}	[24]
	K_{M,NH_4^+}	1.1 mM	[5]
	$K_{M,OG}$	0.32 mM	[5]
	$K_{M,NADPH}$	0.04 mM	[5]
	$K_{M,E}$	10.0 mM	[5]
	$K_{M,NADP}$	0.042 mM	[5]
	Keq	1,290 mM^{-1}	[5]

where $K_{0.5}$ represents the half-saturation constant, whose value depends on the OG concentration according to the relationship:

$$K_{0.5} = 0.37 + 0.53\,[\mathrm{OG}]^{1.043} \tag{5}$$

which was fitted from Fig. 2 in [9].

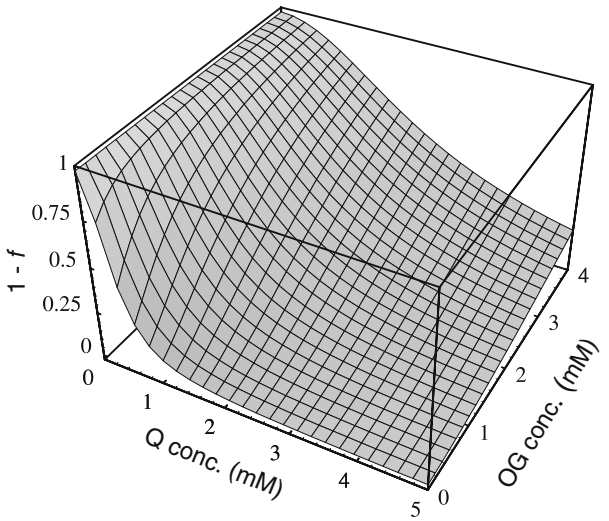

Fig. 2 Three-dimensional representation of the GS activation state $(1-f)$ as a function of Q and OG concentrations

3 Results and Discussion

3.1 Regulation of Glutamine Synthetase

Figure 2 displays the $1 - f$ values (i.e., the fraction of GS activity) obtained for different OG and Q concentrations. To avoid restrictions on $K_{0.5}$ values, we developed our differential equation coupled model in a way that OG (as well as NH_4^+) concentration is variable. In addition, the present model did not include subnetworks, given that reactions catalyzed by UT/UR and AT/AR are contained in effective form in Eq. 4, which relates the OG and Q concentrations. This allowed a more direct and simple calculation of regulation effects.

In the following, we will compare the behavior of the systems with regulated or unregulated GS by multiplying or not [GS] by $(1 - f)$. For brevity, we will refer to these cases as regulated and unregulated systems, respectively.

3.2 Steady State Fluxes Trough the Regulated and Unregulated Systems

As first approximation, we assessed whether, by maintaining the external fluxes J_1 and J_2 unrestricted and equal to 1 mM min^{-1}, and first order output kinetic constants k_6 and k_7 equal to 1 min^{-1}, a steady state for the other fluxes and metabolite concentrations was obtained. Under this situation, the magnitude of all internal fluxes J_3, J_4, and J_5, as well as J_6 and J_7 external fluxes, did not change with time, as expected for the steady state regime. We also observed that, for the cyclic topology, internal fluxes J_4 and J_5 were higher in the unregulated system – i.e. when f was set as 0, irrespective of the OG and Q concentrations – than in the regulated system—where the fractional activity of GS was obtained by multiplying J_4 by $(1 - f)$. However, J_3 was lower in the unregulated system, in agreement with previous results [5], while external fluxes J_6 and J_7 were almost unchanged between the regulated and unregulated systems. To confirm that these differences were due to GS regulation, we obtained the $(1 - f)$ value at steady state, which in the present conditions was approximately 0.13. We then multiplied J_4 in the unregulated system by this value and obtained exactly the same curves as in the regulated system. In contrast to the cyclic topology, no flux changes between regulated or unregulated systems were observed for the linear topology.

When GDH amounts were varied between 0.1 and 3 times the default concentration, J_6 and J_7 also did not change. Instead, these flux values were very sensitive to changes in the input J_1 and J_2 values. In this sense, almost all flux control is at the substrate inputs. Therefore, this constancy in boundary flux injection [15] could be too stringent for the system to allow some study of the flux control exerted by the enzymes internal to the pathway. To relax this stringency in order to transfer some flux control to J_i, we leave only the limitation that absolute values of $J_1 = J_2 = J_7$. With this new setting, we again varied the concentration of GDH and studied its effects on J_6 and J_7 in the regulated and unregulated systems, with both pathway topologies. Since both fluxes had exactly the same values, in the following, we show only the results obtained with J_6, because this represents the releasing step in the synthesis of the final product in the linear topology (Fig. 1). Interestingly, as observed in Fig. 3, J_6 was always higher in the regulated system where GS, the enzyme responsible for its synthesis, was 53% inactivated by adenylylation. A higher E concentration is not surprising since it is a substrate of GS, and therefore lowering the enzyme activation state would lead to substrate accumulation. However, the higher Q production is not as predictable, since this amino acid is a product of GS. The higher Q

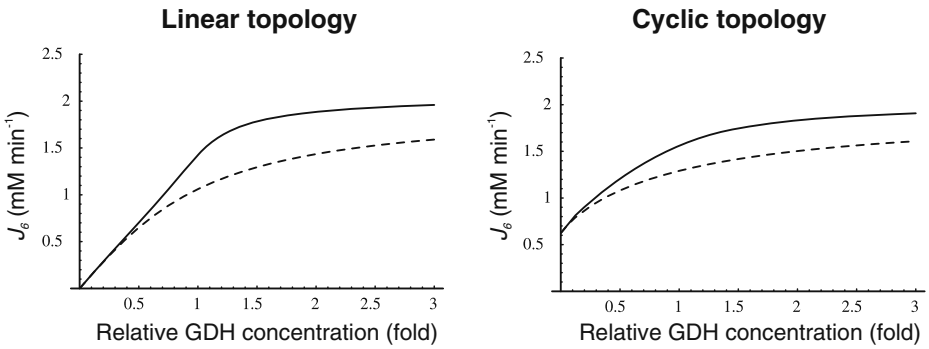

Fig. 3 J_6 as a function of GDH concentrations, expressed as fold-concentration relative to the default GDH concentration (8 μM) for both pathway topologies. *Continuous line*, regulated system; *dashed line*, unregulated system

production was due to the combination of higher NH_4^+ and E concentrations, which more than compensated for the GS partial inactivation, and indeed, it was this inactivation that led to those levels of NH_4^+ and E concentration rising in the first place. Since this rise was also obtained with different system settings (different GDH concentrations, external kinetic constants, or initial metabolite concentrations), this behavior is a system property and not an outcome obtained by chance with a particular setting. At least part of this system behavior could be attributed to the ultrasensitivity of GS regulation. In this regard, GS regulation potentiates E and Q production even when NH_4^+ influx is not limiting, and the OG/Q relationship is low.

The flux control coefficient [17] of GDH on J_6 was more than twofold higher in the linear than in the cyclic topology (Table 2), pointing out that (1) the cyclic topology was more robust in maintaining E and Q production levels against small changes in the amount of GDH in the vicinity of its default concentration and (2) pathway control is transferred to GDH when GOGAT activity is omitted. In addition, pathway control by GDH was almost complete in the linear topology at GDH concentrations up to 4 μM, in agreement with a recent study where GOGAT null mutants were spontaneously reverted by GDH expression mutants that accumulated 2–5 times more GDH than the parental strain [18]. Since the GDH default concentration employed by us is quite high (Table 1), such reversion might be explained if the wild-type GDH concentration was around 1–4 μM, considering that regulation operated normally (Fig. 3).

As observed in Fig. 3, J_6 values tended to a plateau as GDH concentrations increased. Therefore, we also tested further increases in GDH up to 200 times the default concentration, and confirmed that even at these high GDH values there were no changes in J_6 once the plateau was reached. This behavior indicates that, beyond a GDH concentration threshold, large fluctuations in enzyme amounts can be tolerated by the metabolic network without compromising the balance among metabolic fluxes, especially in the cyclic topology.

Table 2 Flux control coefficients of 8 μM GDH on J_6

	GS reg.	GS unreg.
Linear topology	0.94	0.57
Cyclic topology	0.34	0.24

Values for J_7 were exactly the same

Bacterial cell cultures are not completely homogeneous even when cells are clonal and culture conditions are held constant [19] . In a study on individual bacterial swimming, it was estimated that protein levels among individual cells may fluctuate 10% around the mean value for the culture [20]. Our results suggest that this observation could be extended to central metabolism as well.

Calculated steady-state NH_4^+, OG, E, and Q concentrations are shown in Table 3. They agree with those previously reported, and interestingly, NH_4^+ and OG concentrations spontaneously tended to similar values as experimental estimates from previous studies of this pathway in wild-type cells under N-limitation [5, 21]. Nevertheless, it has to be kept in mind that this model only deals with the pathway schematized in Fig. 1 and ignores other pathways such as the tricarboxylic acid cycle or the protein degradation and amino acid recycling, both of which also determine the cellular concentrations of OG, E, and Q, or the use of E to balance intracellular K^+.

3.3 System Responses to Depletion of NH_4^+ External Concentration

Fluctuations in environmental N source are often experienced by bacteria. Among these fluctuations, source depletion occurs when bacteria grow without a continuous provision of the nutrient. To assess the effects of source depletion caused by bacterial growth, we proposed J_1 as a time function $e^{-\alpha t}$ where α is the duplication constant, which, for a 40 min duplication time, was $(\ln 2/40)$ min^{-1}. We choose this law for the initial value $J_{1,0} =$ 1 mM min^{-1}.

We analyzed the system responses in 20-min simulations, thus encompassing half cell generation at the set duplication time. When the external N-source was decaying and the C-source was maintained unlimited by giving J_2 a constant value of 1 mM min^{-1}, differences in internal and external fluxes between regulated and unregulated systems were surprisingly small (not shown). Nevertheless, such differences could be highlighted by diminishing k_6 from 3.0 to 1.0. In the linear topology, J_3 and J_4 diminished, following NH_4^+ depletion, again with small differences between regulated and unregulated systems (Fig. 4). In contrast, in the cyclic topology, J_3 was higher in the regulated system during the first 20 min, while the contrary trend was observed for J_4 and J_5, which were higher in the unregulated system. This result indicates that the regulated system provides a better energy usage for these biosynthetic processes, as suggested by previous physiological experiments [10, 11]. Metabolite export also showed different behaviors. In the unregulated system, J_6 was always a little lower than in the regulated one, while J_7 was higher in the regulated system, for both topologies, both J_e being very similar between linear and cyclic topologies despite the above-mentioned differences in J_i. Differences in J_e between regulated and unregulated systems were smaller in the cyclic topology.

Table 3 Steady state metabolite concentrations (mM) $k_6 = 3$, $k_7 = 1$

Metabolite	Linear topology		Cyclic topology	
	GS regulated	GS unregulated	GS regulated	GS unregulated
E	1.42	1.06	1.56	1.29
Q	0.47	0.35	0.52	0.43
OG	0.30	0.47	0.23	0.36
NH_4^+	0.02	0.01	0.03	0.01

Initial concentrations E= 1, Q= 1, OG= 1, N= 1

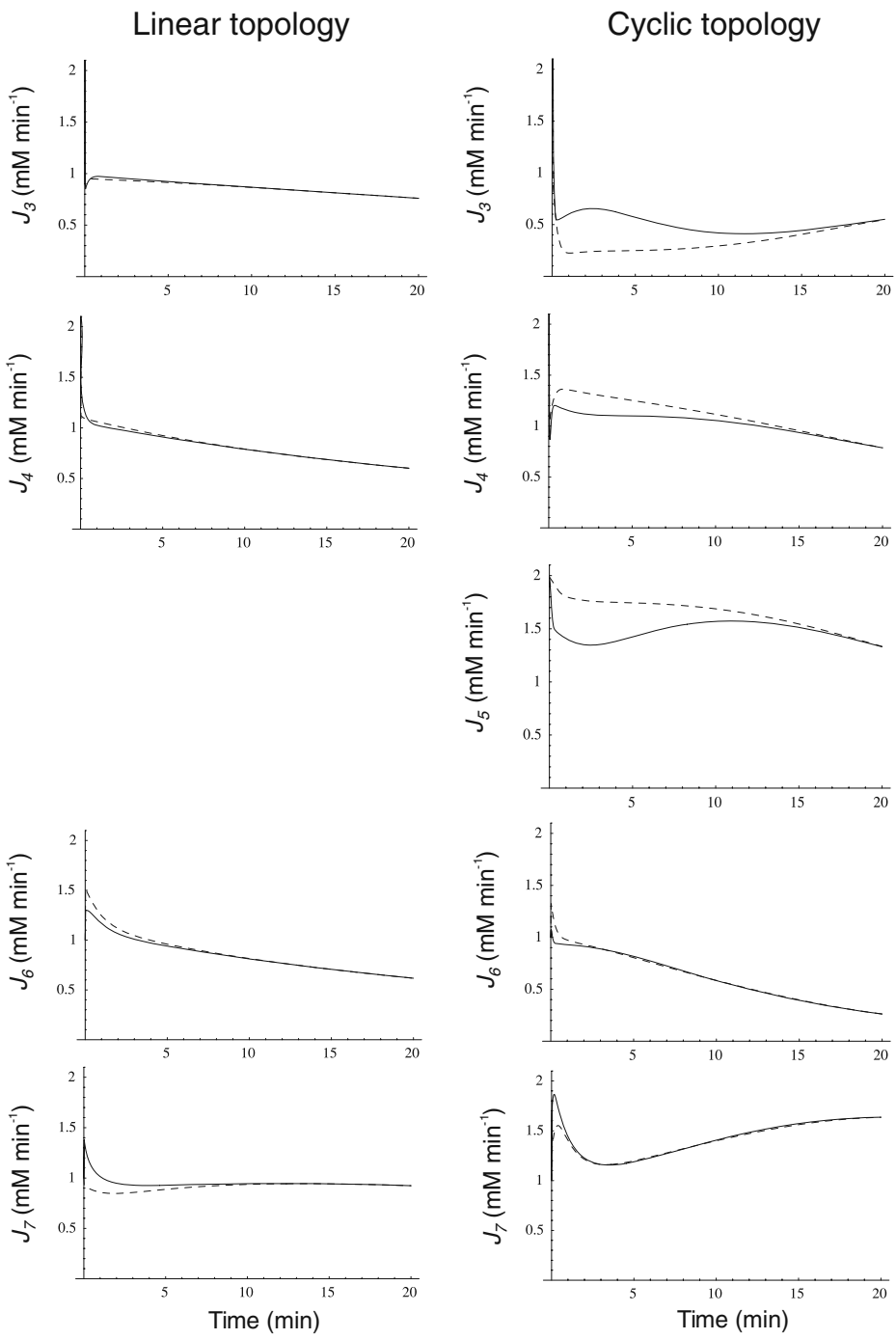

Fig. 4 J_i and J_e as a function of time when the N-source was diminishing at a rate defined by $J_{1,0}e^{-\alpha t}$ for both pathway topologies. *Continuous line*, regulated system; *dashed line*, unregulated system

Since these different behaviors between the regulated and unregulated systems depended on the k_6 and k_7 values, we investigated the relationship between these values, the regulation, and the differences in J_i. Regulation kinetics depended on k_6 and k_7 values. For instance, when k_7 was 1, $(1 - f)$ approached the maximum value of 1 earlier, as k_6 values were higher (Fig. 5). A similar behavior was observed with different k_7 values (not shown). This means that, as long as k_6 is comparatively higher than k_7, Q leaves the system faster, and therefore, its accumulation is lowered, thus increasing the OG/Q relationship earlier. To better study this effect on internal J_i fluxes, we integrated the differences between the $J_{i,\text{unregulated}} - J_{i,\text{regulated}}$ (integrated ΔJ_i) for different $(k_7 - k_6)$ values. This study was restricted to a 10-min simulation for the linear and cyclic topologies, since it is during this period that significant regulation takes place (Fig. 5). In Fig. 6, it is shown that differences in J_i between the unregulated and regulated systems were always higher for the cyclic topology, as observed by comparing the scale differences in $\int \Delta J_i$ axes. Furthermore, the linear topology did not show a defined trend as the cyclic topology did. In the cyclic topology J_3 values were higher for the regulated system, while J_4 and J_5 were always higher for the unregulated one, with these differences approaching minimal but positive values when k_6 exceeded k_7 but exponentially increasing as k_6 approached k_7. By fitting data in Fig. 6, we found that, for the cyclic topology, the relationship between flux differences and $(k_7 - k_6)$ may be represented as:

$$\int \Delta J_i = c + ae^{b(k_7 - k_6)}, \tag{6}$$

with b values around 2. This indicated that, for any infinitesimal increment in the difference $(k_7 - k_6)$, the corresponding $\int \Delta J_i$ was duplicated. Since k_6 and k_7 represent the cellular metabolic demands of Q and E, respectively, this observation indicates that regulation effects depend also on the general metabolic context. In particular, in vivo E concentration was regarded as more than enough to fulfill cell N demands, having an additional role in counterbalancing intracellular K^+ concentration [22]. If we consider this role of E as an additional output, this might configure a situation where, most frequently, $k_7 \geq k_6$, i.e., in the positive range of the $(k_7 - k_6)$ axis.

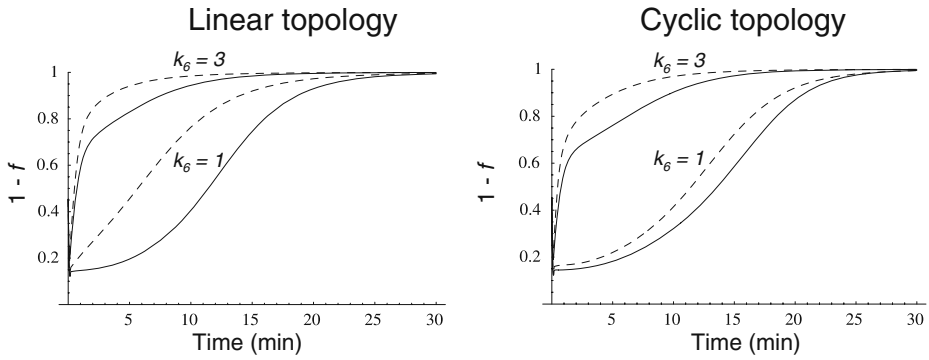

Fig. 5 GS fractional activity $(1 - f)$ due to adenylylation of a fraction f of GS subunits as a function of time when the N-source was diminishing at a rate defined by $J_{4,0}e^{-\alpha t}$ for both pathway topologies, with $k_7 = 1$ and different k_6 values. *Continuous line*, GS 240 nM; *dashed line*, GS 2,400 nM

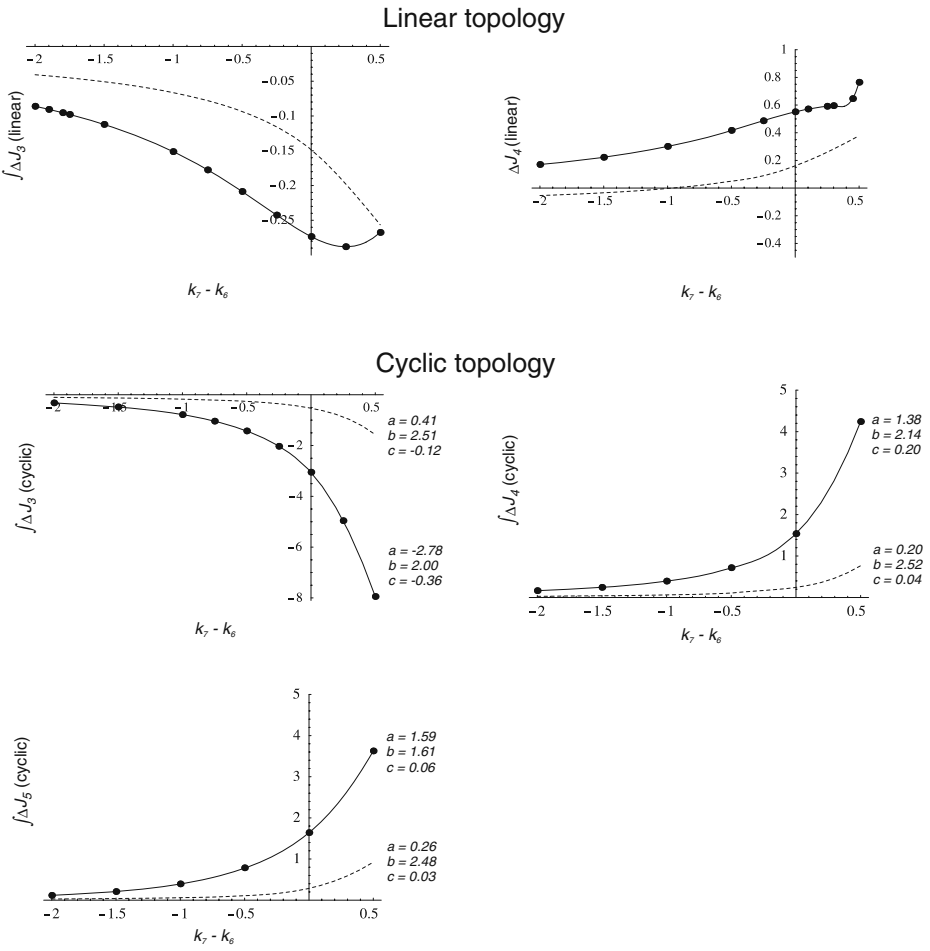

Fig. 6 Integrated ΔJ_i (in nonregulated minus regulated systems) as function of the difference $k_7 - k_6$ calculated for the first 10-min simulation, when the N-source was diminishing at a rate defined by $J_{1,0}e^{-\alpha t}$. *Dots*, calculated values from the simulations. *Lines*, interpolations for the linear topology (*upper panel*) or resolution of $\int \Delta J_i = c + ae^{b(k_7 - k_6)}$ for the cyclic topology (*lower panel*) with values for a, b, and c as indicated. *Continuous line*, GS 240 nM; *dashed line*, GS 2,400 nM

Another known effect of N-source depletion in *E. coli* is stimulation of *gln*A gene expression [1] whereby GS total concentration rises. To see whether such an enzyme concentration change may affect GS adenylylation effects, we repeated the above studies with 10 times higher total GS concentration (dashed lines in Figs. 5 and 6). After raising GS concentration, we saw that regulation followed the same trend but similar levels of total activation were achieved earlier, both in the linear and cyclic pathways. As a consequence, the response to regulation with different k_6 and k_7 values also followed the same trend as with default GS concentration, but the magnitudes of differences in J_i between unregulated and regulated systems were lowered. Interestingly, in the cyclic topology, the same law fitted the relationship between $\int \Delta J_i$ and $(k_7 - k_6)$ with b values in the same order as with default GS concentration (Fig. 6).

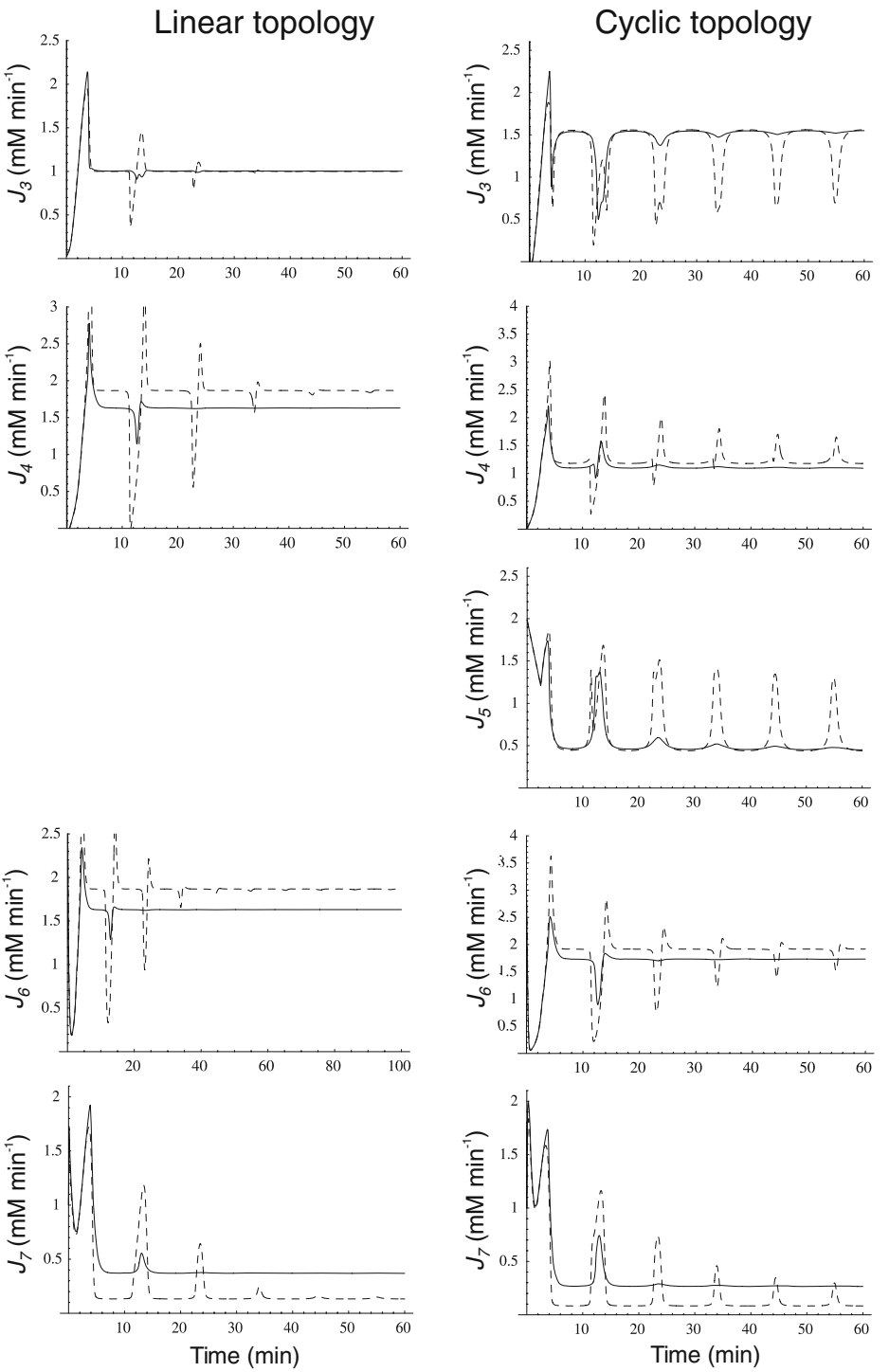
Linear topology
Cyclic topology
J_3 (mM min^{-1})
J_4 (mM min^{-1})
J_5 (mM min^{-1})
J_6 (mM min^{-1})
J_7 (mM min^{-1})
Time (min)
Time (min)

◀ **Fig. 7** J_i and J_e as a function of time when the N-source was oscillating as defined by $J_{1\text{Max}} \sin^2 \omega t$ where $\omega = 0.3$ for both pathway topologies. *Continuous line*, regulated system; *dashed line*, unregulated system

3.4 System Responses to Oscillations in NH_4^+ External Concentration

In addition to depletion, the external N source could be perturbed in different ways, for instance, oscillating as a consequence of cycles of nutrient input pulses and/or washes. To introduce oscillations, we multiplied J_1 by $J_{e,\text{Max}} \sin^2 \omega t$, where $\omega = 0.3$, with $J_{e,\text{Max}} = 2.6$, leaving J_2 at a constant value of 1 mM min^{-1}.

When external NH_4^+ was subjected to oscillation between 0 and 2.6 mM with a period of 10 min, internal and external fluxes varied following N-source oscillations in the unregulated system, while the same fluxes rapidly stabilized after a few oscillations in the regulated system. This trend was more pronounced in the cyclic than in the linear topology (Fig. 7). In the cyclic topology, J_4 and J_5 showed bursts of activity in the unregulated system that coincided with deep valleys in J_3. Thus, regulation avoided these peaks of energy consumption for E synthesis. Furthermore, J_7 tended to almost zero in the unregulated system with both topologies while significant E provision was sustained in the regulated system, with this trend being more remarkable when the difference between k_6 and k_7 decreased, as observed previously for N-depletion (not shown). This behavior of J_7 may be explained by the decreased amount of NH_4^+ consumption by regulated GS, which "keeps" some NH_4^+ from the previous peak in the system, thus controlling the NH_4^+ availability better during the next valley. Therefore, an important role of GS regulation under conditions of external N-source uncontrolled variation (as should be the most frequent case in natural bacterial environments) might be to control the internal cell availability of NH_4^+ as a raw material for amino acid biosynthesis in order to decouple this process from external source fluctuations.

4 Concluding Remarks

A prominent feature suggested by simulations carried out in this article is that GS regulation provided higher robustness to internal fluxes and outcome external fluxes against changes in enzyme concentrations or N-source perturbations. This was especially important for J_7 when N oscillated (Fig. 7), the unregulated system being very weak in sustaining E production under these conditions. The quality of this regulation seems to reside in the partial inhibition of a highly efficient enzyme (specificity constant for $NH_4^+ = 3.9$ 10^5) through an ultrasensitive mechanism. Both characteristics (enzyme efficiency and ultrasensitivity of the regulation cascade) allow rapid responses to the stimulus.

As a general trend, the responses to N-source perturbations were more important in the cyclic than in the linear topology. In this regard, the GS-GOGAT cycle might add sensitivity to the GS regulation response [17].

Acknowledgements This work was supported by Universidad Nacional de La Plata, Argentina (UNLP). AL is a researcher at Consejo Nacional de Investigaciones Científicas y Tecnológicas, Argentina. AM is a Professor at UNLP.

References

1. Reitzer, L.J.: Ammonia assimilation and the biosynthesis of glutamine, glutamate, aspartate, asparagine, L-alanine, and D-alanine. In: Neidhardt, E.A. (ed.) *Escherichia coli* and *Salmonella*: Cellular and Molecular Biology, pp. 391–407. ASM, Washington, D.C. (1996)
2. Rhee, S.G., Chock, P.B., Stadtman, E.R.: Regulation of *Escherichia coli* glutamine synthetase. Adv. Enzymol. Relat. Areas Mol. Biol. **62**, 37–92 (1989)
3. Shapiro, B.M., Kingdon, H.S., Stadtman, E.R.: Regulation of glutamine synthetase, VII. Adenylyl glutamine synthetase: a new form of the enzyme with altered regulatory and kinetic properties. Biochemistry **58**, 642–649 (1967)
4. Mura, U., Chock, P.B., Stadtman, E.R.: Allosteric regulation of the state of adenylylation of glutamine synthetase in permeabilized cell preparations of *Escherichia coli*. Studies of monocyclic and bicyclic interconvertible enzyme cascades, in situ. J. Biol. Chem. **256**, 13022–13029 (1981)
5. Bruggeman, F.J., Boogerd, F.C., Westerhoff, H.V.: The multifarious short-term regulation of ammonium assimilation of *Escherichia coli*: dissection using an *in silico* replica. FEBS J. **272**, 1965–1985 (2005)
6. Ninfa, A.J., Atkinson, M.R: PII signal transduction proteins. Trends Microbiol. **8**, 172–179 (2000)
7. Jiang, P., Peliska, J.A., Ninfa, A.J.: Enzymological characterization of the signal-transducing uridylyltransferase/uridylyl-removing enzyme (EC 2.7.7.59) of *Escherichia coli* and its interaction with the PII protein. Biochemistry **37**, 12782–12794 (1998)
8. Ortega, F., Acerenza, L., Westerhoff, H.V., Mas, F., Cascante, M.: Product dependence and bifunctionality compromise the ultrasensitivity of signal transduction cascades. Proc. Natl. Acad. Sci. U. S. A. **99**, 1170–1175 (2002)
9. Mutalik, V.K., Shah, P., Venkatesh, K.V.: Allosteric interactions and bifunctionality make the response of glutamine synthetase cascade system of *Escherichia coli* robust and ultrasensitive. J. Biol. Chem. **278**, 26327–26332 (2003)
10. Helling, R.B.: Why does *Escherichia coli* have two primary pathways for synthesis of glutamate? J. Bacteriol. **176**, 4664–4668 (1994)
11. Helling, R.B.: Speed versus efficiency in microbial growth and the role of parallel pathways. J. Bacteriol. **184**, 1041–1045 (2002)
12. Dixon, M., Webb, E.C.: Enzymes. Academic, New York (1979)
13. Miller, R.E., Stadtman, E.R.: Glutamate synthase from *Escherichia coli*. An iron-sulfide flavoprotein. J. Biol. Chem. **247**, 7407–7419 (1972)
14. Beard, D.A., Babson, E., Curtis, E., Qian, H.: Thermodynamic constraints for biochemical networks. J. Theor. Biol. **228**, 327–333 (2004)
15. Qian, H., Beard, D.A.: Thermodynamics of stoichiometric biochemical networks in living systems far from equilibrium. Biophys. Chem. **114**, 213–220 (2005)
16. Qian, H., Beard, D., Liang, S.D.: Stoichiometric network theory for nonequilibrium biochemical systems. Eur. J. Biochem. **270**, 415–421 (2003)
17. Fell, D.: Understanding the Control of Metabolism. Portland, London (1996)
18. Yan, D.: Protection of the glutamate pool concentration in enteric bacteria. Proc. Natl. Acad. Sci. U. S. A. **104**, 9475–9480 (2007)
19. McAdams, H.H., Arkin, A.: Stochastic mechanisms in gene expression. Proc. Natl. Acad. Sci. U. S. A. **94**, 814–819 (1997)
20. Levin, M.D., Morton-Firth, C.J., Abouhamad, W.N., Bourret, R.B., Bray, D.: Origins of individual swimming behavior in bacteria. Biophys. J. **74**, 175–181 (1998)
21. Senior, P.J.: Regulation of nitrogen metabolism in *Escherichia coli* and *Klebsiella aerogenes*: studies with the continuous culture technique. J. Bacteriol. **123**, 407–418 (1975)
22. Yan, D., Ikeda, T.P., Shauger, A.E., Kustu, S.: Glutamate is required to maintain the steady-state potassium pool in *Salmonella typhimurium*. Proc. Natl. Acad. Sci. U. S. A. **93**, 6527–6531 (1996)
23. Woolfolk, C.A., Shapiro, B., Stadtman, E.R.: Regulation of glutamine synthetase. I. Purification and properties of glutamine synthetase from *Escherichia coli*. Arch. Biochem. Biophys. **116**, 177–192 (1966)
24. Sakamoto, N., Kotre, A.M., Savageau, M.A.: Glutamate dehydrogenase from *Escherichia coli*: purification and properties. J. Bacteriol. **124**, 775–783 (1975)